Molecular Therapy
Nucleic Acids
Original Article

Inhibition of the LINE1-derived *MET* transcript induces apoptosis and oncoprotein knockdown in cancer cells

Umberto Miglio,[1,8] Enrico Berrino,[1,2,8] Daniele Avanzato,[3,6] Ivan Molineris,[4] Valentina Miano,[5,7] Melissa Milan,[1] Letizia Lanzetti,[1,3] Eugenio Morelli,[1,3] James M. Hughes,[1] Michele De Bortoli,[5] Anna Sapino,[1,2,9] and Tiziana Venesio[1,9]

[1]Candiolo Cancer Institute, FPO-IRCCS, Candiolo, 10060 Candiolo, TO, Italy; [2]Department of Medical Sciences, University of Torino, 10126 Torino, Italy; [3]Department of Oncology, University of Torino Medical School, 10043 Orbassano, TO, Italy; [4]Department of Life Sciences and System Biology and MBC, University of Torino, 10123 Torino, Italy; [5]Department of Clinical and Biological Sciences, University of Torino, 10043 Orbassano, TO, Italy

The expression of intragenic long interspersed nuclear elements 1 (LINE1s) can generate chimeric sequences disrupting host gene transcription. Among these, L1-*MET*, within *mesenchymal epithelial transition* (*MET*) oncogene, is particularly interesting, as its expression has been associated with the acquisition of tumorigenic phenotypes and cancer progression. We investigated the effects of targeting L1-*MET* in eight cancer cell lines derived from breast, lung, and gastrointestinal cancers, as well as in non-transformed human fibroblasts and lymphocytes, using specifically developed modified antisense oligonucleotides. Inhibition of L1-*MET* resulted in decreased cell viability, increased apoptosis, and gene expression profile reprogramming in cancer cells, including significant downregulation of MET and epidermal growth factor receptor (EGFR) proteins. These effects were related to the L1-*MET*/*MET* expression levels and the type of cellular addiction, with pronounced impacts in cells harboring *MET* gene amplification and *EGFR*-activating mutations. They were also detectable, though less pronounced, in cancer cells with steady-state levels of MET and EGFR proteins or addiction to other oncogenes. We demonstrate that targeting L1-*MET* can knockdown MET and EGFR protein. The restricted expression of L1-*MET* to cancer cells suggests that its inhibition could be an effective strategy to induce death in oncogene-addicted tumor cells and offers a potential means to overcome the limitations of conventional targeted therapies.

INTRODUCTION

Numerous strategies have been developed to identify therapies that selectively target cancer cells while sparing normal cells and preventing the onset of treatment resistance. However, these efforts often fall short due to the challenges in identifying "private" molecular targets and simultaneously addressing the mutational heterogeneity of the cancer cells. Intragenic long interspersed nuclear elements 1 (LINE1 or L1) have emerged as promising candidates for targeted therapy, owing to their ability to modulate the expression of their host cancer genes through the generation of chimeric transcripts.[1] These transcripts are typically activated by hypomethylation of their L1 antisense promoters (ASPs).[2–5] Among the antisense chimeric sequences identified,[6] the fusion isoform originating from the L1 element located in the second intron of the *mesenchymal epithelial transition* (*MET*) gene (L1-*MET*)[7,8] is of particular interest. Aberrant activation of L1-*MET* has been implicated in the acquisition of cancerous phenotypes. Previous studies have documented the involvement of L1-*MET* in the development of bladder[9] and hepatocellular carcinomas[10] as well as in the progression of colorectal cancer.[11,12] More recently, we demonstrated that high levels of L1-*MET* expression are characteristic of a subset of triple-negative and high-grade breast carcinomas.[13]

The precise role of L1-*MET* in cancer, whether through its modulation of *MET* (a well-known oncogene that contributes to tumor progression and metastasis)[14] or independent of *MET* regulation, remains a topic of debate. Similar to long non-coding RNAs (lncRNAs),[15] L1-*MET* generates splicing variants that result in nonfunctional peptides. Notably, L1-*MET* isoforms can include up to the last exon of canonical *MET* transcript, yielding a total length of about 3,000 base pairs. Although stable L1-*MET* transcripts have been identified in both the nucleus and the cytoplasm of cancer cells, they do not form stable truncated protein(s).[13]

The relationship between *L1-MET/MET* remains poorly understood, though evidence suggests transcriptional interference between the

Received 27 August 2024; accepted 27 March 2025;
https://doi.org/10.1016/j.omtn.2025.102529.

[6]Present address: Department of Veterinary Sciences, University of Torino, 10095 Grugliasco, TO, Italy

[7]Present address: Tagomics Ltd, Little Abington, Cambridge, CB21 6GP, UK

[8]These authors contributed equally

[9]These authors contributed equally

Correspondence: Tiziana Venesio, Candiolo Cancer Institute, FPO-IRCCS, Candiolo, 10060 Candiolo, TO, Italy.
E-mail: tiziana.venesio@ircc.it

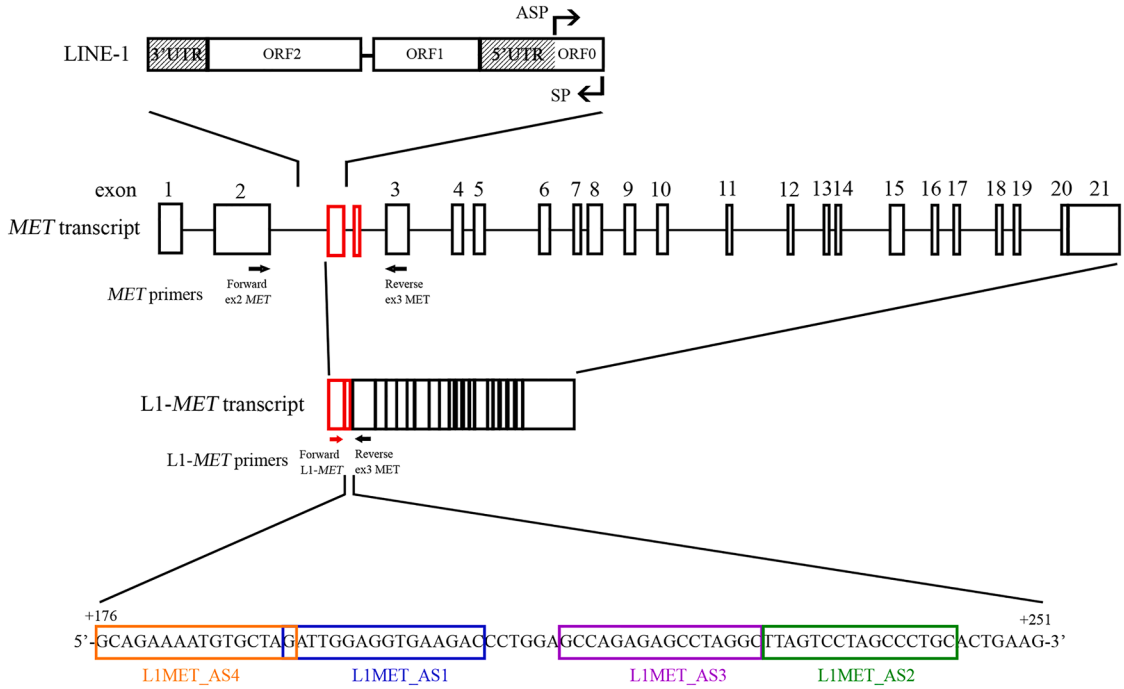

Figure 1. Graphical representation of the L1-*MET* transcript and its selected targeting ASO/gapmers

MET intron 2 harbors a L1 inserted in the opposite orientation of *MET* with the sense promoter (SP) and the 5′-UTR encompassing the ORF0 sequence comprising the antisense promoter (ASP) leading to the L1-*MET* transcript. The first methionine of ORF0 maps to intronic nucleotide g.56654A (c.1201-7610A) of *MET* gene and its first nucleotide is taken as +1 of the L1-*MET* reference numbering. The L1-*MET* sequence, spanning nucleotides +176 and +251, contains the target region (76 bp) for ASO/gapmer targeting (NCBI: NM_000245.4); ORF and ASO/gapmer targeting regions are reported in square red; each selected ASO/gapmer is labeled with a different color. Forward primers for *MET* mRNA and L1-*MET* transcript quantification are mapped on *MET* exon 2 and on the ORF0 region, respectively, whereas the common reverse primer is localized on *MET* exon 3.

L1-*MET* transcript and MET protein.[16] Supporting this, our previous work revealed that in a subset of aggressive breast cancers, a high L1-*MET*/*MET* transcript ratio was associated with the absence of MET protein expression, suggesting a potential interplay between the two transcripts in at least some tumors.[13]

Building on these findings, we investigated the effects and potential therapeutic exploitation of L1-*MET* silencing by developing unique modified antisense oligonucleotides (ASOs),[17] designed to specifically inhibit L1-*MET*.

We examined the impact of L1-*MET* silencing in a panel of breast, lung, and gastrointestinal cancer-derived cells, each characterized by varying levels of L1-*MET*/*MET* transcripts and different oncogenic dependencies. The consequences of L1-*MET* inhibition were assessed through its effects on proliferation, apoptosis, MET protein expression and its phosphorylation, and transcriptional expression profile.

RESULTS

In silico characterization of modified ASOs targeting L1-*MET*

To investigate the effect of L1-*MET* silencing, we employed ASOs specifically designed to target the L1-*MET* transcript. The L1-ORF0 sequence in *MET* intron 2 contains the ASP which leads to the L1-*MET* transcript (Figures 1 and S1). We identified a 76 bp fragment, spanning nucleotides +176 and +251 in L1-*MET*, as the most suitable private target sequence (NCBI Gene Bank accession # NM_000245.4) (Figures 1 and S1). Subsequent, *in silico* analysis pinpointed four out of eleven potential ASOs: L1-MET_AS1, complementary to nucleotides +191 to +206; L1-MET_AS2, targeting nucleotides +229 to +245; L1-MET_AS3, targeting nucleotides +213 to +228; and L1-MET_AS4, complementary to nucleotides +176 to +191 (Figures 1 and S1; Table 1).

We then evaluated the efficiency of these ASOs based on several parameters.[18] First, we used the sRNA software sFOLD to predict their secondary structures and determine their level of thermostability. Three of the ASOs (L1-MET_AS1/2/4) exhibited low-fold propensity while L1-MET_AS3 showed a distinct hairpin structure. To further assess ASO efficiency, we calculated the Gibbs free energy (ΔG), which represents the energy released during the folding of a completely unfolded molecule. Lower ΔG levels are typical of molecules with a high propensity for self-folding, whereas fewer hydrogen bonds within the ASO indicate a reduced tendency to form secondary structures. In this context, an ASO with a higher (more positive) ΔG is considered more efficient. The ΔG analysis confirmed that L1-MET_AS3 was the least stable. L1-MET_AS1 emerged as the

Table 1. Sequences, ΔG levels, and position on L1-*MET* transcript of the eleven identified ASOs

ASO ID	Sequence 5′->3′	ΔG ASO	Base pair position on L1-*MET*
L1MET_AS1[a]	GUCUUCACCUCCAAUC[a]	2.5	191–206
L1MET_AS2[a]	GCAGGGCUAGGACUAA[a]	0.6	229–245
L1MET_AS3[a]	GCCUAGGCUCUCUGGC[a]	−2.7	213–228
L1MET_AS4[a]	CUAGCACAUUUUCUGC[a]	0	176–191
L1MET_AS5	CUCCAAUCUAGCACAU	3.4	183–198
L1MET_AS6	ACCUCCAAUCUAGCAC	3.1	185–200
L1MET_AS7	CUAGGCUCUCUGGCUC	−1.8	211–226
L1MET_AS8	CUAAGCCUAAGGCUCUC	−2.7	217–232
L1MET_AS9	GUGCAGGGCUAGGACU	1.1	231–246
L1MET_AS10	AGUGCAGGGCUAGGAC	1.1	292–307
L1MET_AS11	CUUCAGUGCAGGGCUA	0.2	236–251

[a]The four selected gapmers (L1MET_AS1/2/3/4).

most stable (ΔG = 2.5), while L1-MET_AS2/4 showed intermediate values (ΔG = 0.6 and 0.0, respectively) (Table 1). Next, we examined the sequence composition for T stretches and palindrome sequences, which are detrimental to ASO activity. L1-MET_AS4 displayed a 4T stretch in the hairpin loop, significantly impairing its potential effectiveness. Finally, we evaluated the heteroduplex formed by the ASO and the target RNA by analyzing the entire L1-*MET* sequence using the sRNA algorithm in sFOLD. Overall, L1-MET_AS1 and AS2 targeted the most favorable regions. Due to the poor sequence characteristics and thermal stability, we excluded L1-MET_AS4 from further study, although L1-MET_AS3 was retained despite its predicted low stability (Figure S2).

No potential off-target transcripts for the selected ASOs were identified using transcriptome searches with NCBI blastn (https://blast.ncbi.nlm.nih.gov/Blast.cgi) and ENSEMBL blastn (https://www.ensembl.org/Homo_sapiens/Tools/Blast), even when a single nucleotide mismatch was considered.

Corresponding gapmers of the selected ASOs were then developed. Gapmers are ASOs formed by a DNA central fragment and RNA-like segments on both sides of the sequence. They are designed to hybridize to a target piece of RNA and silence the gene through the induction of RNase H cleavage.[19,20] They are known to work effectively at low concentrations on lncRNA-like sequences regardless of their intracellular localization.[21] To improve the affinity in targeting and stably inhibiting L1-*MET*, gapmers were locked nucleic acid (LNA) modified, a process in which the 2′-hydroxyl group of the ribose moiety is linked to the 3′ or 4′ carbon atom of the sugar ring thereby forming a bicyclic sugar moiety. This modification was shown to improve the specific and sensitive detection of non-coding RNA and other small RNA molecules.[22] After the introduction of LNA modification, the three selected gapmers were checked *in silico* to test their properties. The gapmer derived from L1-MET_AS1 still resulted in the most efficient one, followed by L1-MET_AS2. The modified gapmers were designated as L1MET_AS1, L1MET_AS2, and L1MET_AS3. Collectively, they were designated L1MET_Gapmers.

Cancer cell models

To study the effects of targeting L1-*MET*, we preliminarily screened several cancer cell lines using quantitative real-time PCR (real-time qPCR) to assess their L1-*MET* and *MET* expression levels. To this purpose, we selected forward primers on *MET* exon 2 and L1-ORF0 region, for *MET* mRNA and L1-*MET* transcript, respectively, combined with a common reverse primer on *MET* exon 3 (Figure 1; Table S1). Relative quantification of both *MET* and L1-*MET* was performed using the ΔCT method, with GAPDH as housekeeper. In addition, L1-*MET/MET* was rationed to obtain the n-fold of expression between the transcripts (Figure 2). Based on this analysis, we identified a panel of cell lines representing variable combinations of L1-*MET/MET* mRNA, including breast cancer (MDA-MB231, BT474, MCF-7, and MDA-MB453), lung cancer (EBC1, A549, and NCI-H1993), and gastrointestinal (GTL16) cancer cells. Human fibroblasts (MRC5) and normal lymphocytes were included as controls (Figure 2). Specifically, EBC1, NCI- H1993, and GTL16 cells exhibited the highest levels of both L1-*MET* and *MET*, followed by A549 cells, which showed moderate levels of both transcripts, and MDA-MB231 cells, which showed a *MET* transcript level similar to A549, but very low level of L1-*MET*. BT474 cells had a fair level of L1-*MET*, but a very low expression of *MET*. Notably, MDA-MB453 cells lacked detectable levels of both transcripts, whereas MCF-7 had almost undetectable *MET* mRNA. Among the controls, the non-transformed fibroblasts (MRC5) were negative for L1-*MET* expression and showed weak *MET* expression, while normal lymphocytes were negative for both transcripts (Figure 2).

The selected cancer cells were further characterized by sequencing and fluorescence *in situ* hybridization (FISH) analysis to verify the presence of specific oncogenic alterations associated with each cell line, as reported in literature and Cancer Cell Line Encyclopedia dataset (https://sites.broadinstitute.org/ccle/). We detected, by sequencing, *EGFR* p.L858R activating mutation in EBC1, *KRAS/BRAF* pathogenic variants in both lung and breast cancer cells (A549, MDA-MB231, and MDA-MB453), and *PIK3CA* mutations in breast cancer-derived cells (MCF-7, MDA-MB453, and BT474) (Figure 2). In addition, we confirmed by FISH the presence of a *MET* whole gene amplification in EBC1, NCI-H1993, and GTL16 cancer cells[23,24] (Figure 2).

The effects of targeting L1-*MET*

We investigated the effects of L1-*MET* targeting by transiently transfecting the cancer cells and the controls using the most effective *in silico* gapmer, L1MET_AS1. We first evaluated different gapmer concentrations (5 nM, 10 nM, and 25 nM) and time (24 h and 48 h after transfection). We chose 25 nM and 24 h as the optimal conditions for the following experiments of L1-*MET* inhibition as 25 nM was the most effective concentration, detectable already after 24 h, without

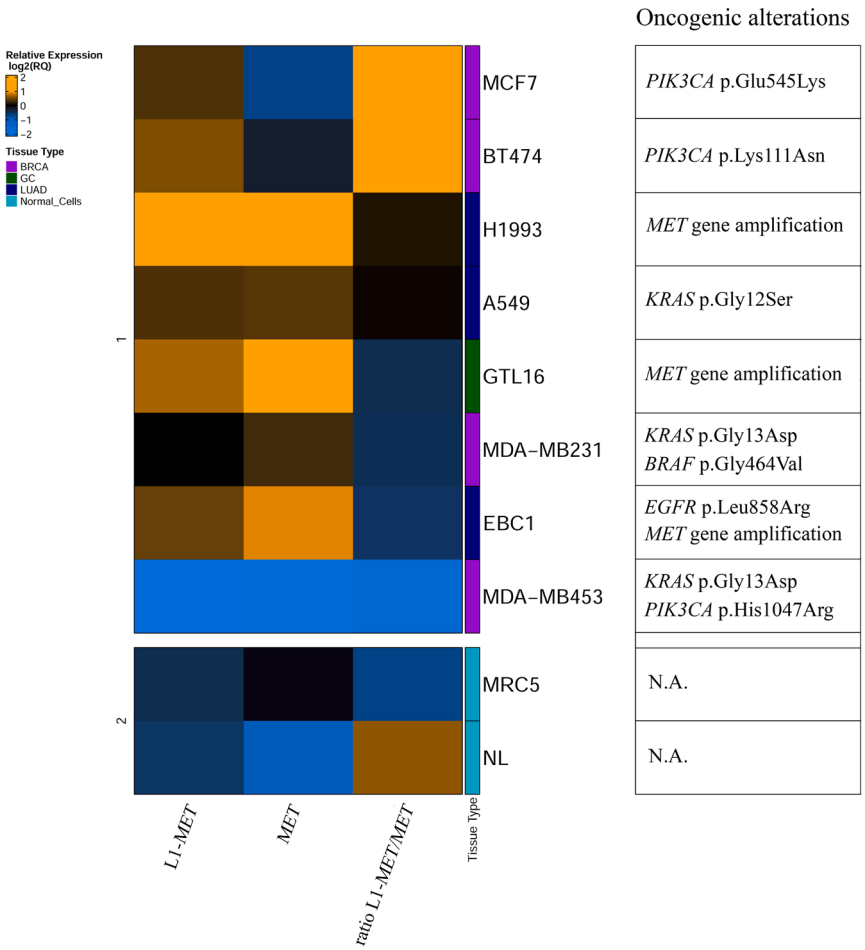

Figure 2. Heatmap showing the expression of L1-*MET*, *MET*, and L1-*MET*/*MET* ratio as measured by real-time qPCR

Relative quantification of both *MET* and L1-*MET* was performed using the ΔCT method, with the GAPDH as housekeeper; L1-*MET*/*MET* was rationed to obtain the n-fold of expression between the transcripts. In the upper left, the color representation of the relative expression, spanning from orange (highest expression) to light blue (no expression). The list of the oncogenic alterations detected in each cancer cell line and the cancer tissue type, from which the cell lines were derived, labeled in different colors, are reported on the right of the heatmap; the list of the tissue types is reported on the upper left, BRCA, breast cancer; GC, gastric cancer; LUAD, lung adenocarcinoma; normal_cells.

any toxicity. We compared L1-*MET* levels in cell lines transfected with L1MET_AS1 *versus* the cell counterpart transfected with scramble gapmers (controls). The L1-*MET* expressing cells exhibited a variable reduction in L1-*MET* levels, ranging between 12% and 81% (Figure 3A). A strong reduction of *MET* mRNA was observed in EBC1, A549, and GTL16 cells (ranging from 57% to 94%), whereas a modest decrease was found in NCI-H1993 cells (16%), and, notably, no change in MDA-MB231 cells, which was associated with a slight decrease of L1-*MET* transcript (14%) (Figures 3A and 3B). In addition, cancer cells with a common *MET* whole gene amplification (EBC1, GTL16, and NCI-H1993) showed a highly variable *MET* mRNA downregulation (16%–94%) (Figure 3B).

We next assessed cell proliferation 24 h after transfection using a cell viability assay. L1-*MET* silencing led to decreased growth in 5 out of 8 cancer cell lines, with strong effects observed in EBC1, A549, and GTL16 cells ($p < 0.0001$, $p = 0.0001$, $p = 0.0003$, respectively) (Figure 3C). A significant, but lower growth reduction was also detected in NCI-H1993 and MDA-MB231 cells ($p = 0.0132$, and $p = 0.0194$, respectively), whereas no significant effects were found in BT474 and MCF-7 breast cancer cells, which expressed L1-*MET*, but had very low levels of *MET* mRNA. Similarly, no changes were observed in MDA-MB453 cells, which lacked detectable levels of both L1-*MET* and *MET* mRNA. As expected, no effects were observed in the control cells (MRC5 and human lymphocytes) (Figure 3C). Notably, the growth impairment correlated with the expression of both L1-*MET* ($p = 0.0437$) and *MET* ($p = 0.0033$), using a cell viability cut-off of −20% as the average value (Figure 3D). However, due to the different expression ranges of L1-*MET* and *MET* mRNA, no association was evidenced when considering the L1-*MET*/*MET* ratio.

To determine whether the reduced proliferation was associated with increased apoptosis, we analyzed the apoptotic index of silenced cells by flow cytometry. At 24 h post-transfection, the cancer cells with the greatest proliferative inhibition (EBC1, A549, and GTL16) also showed an increased percentage of apoptotic cells (ranging between 8% and 35%) compared to their counterparts transfected with scramble gapmers (Figure 4A). In contrast, NCI-H1933 and MDA-MB231 cells did not show increased apoptosis. As expected, no differences were observed between cells transfected with L1MET_AS1 and those transfected with scramble gapmers in the case of

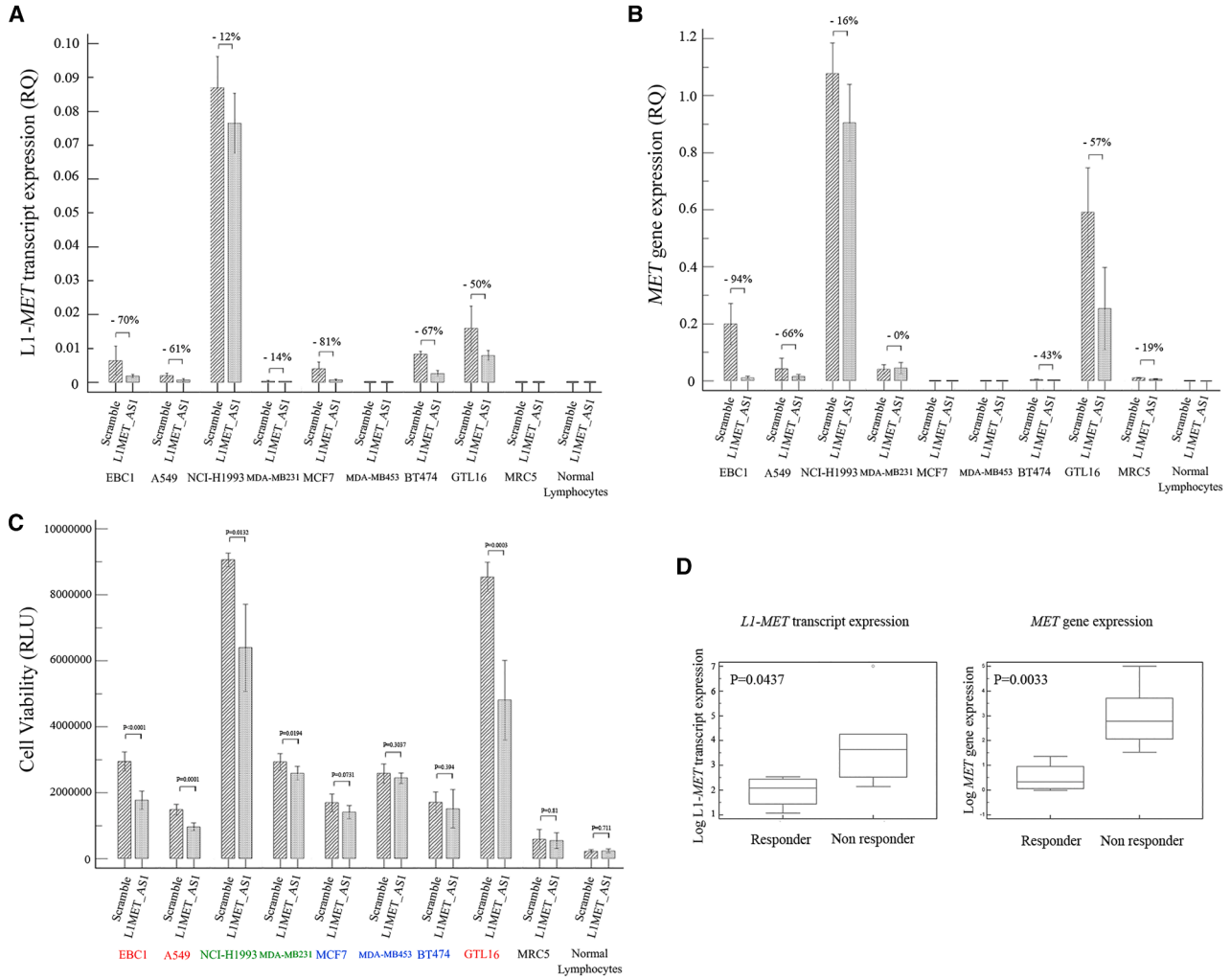

Figure 3. Effects of L1MET_AS1 on the cancer cell panel (EBC-1, A549, NCI-H1993, MDA-MB231, MCF-7, MDA-MB453, BT474, and GTL16) and cell controls (MRC5 and normal lymphocytes) at 24 h after transfection

Bar-plots representing the reduction of the L1-*MET* (A) and *MET* mRNA (B) upon transfection of L1MET_AS1 and scramble gapmers, measured by real-time qPCR analysis. (C) Bar-plot showing viability changes of the cancer cell lines as measured by Cell-titer Glo assay, upon transfection of L1MET_AS1 and scramble gapmers (control). (D) Box-plots reporting the association between growth inhibition and the L1-*MET* ($p = 0.0437$) and *MET* ($p = 0.033$) expression. RQ, relative quantification; RLU, relative light unit; in (A), (B), and (C), data are the mean of at least 3 biological replicates ±SD. Responsive cancer cells, labeled in red; low-responsive cancer cells, labeled in green; non-responsive cancer cells, labeled in blue.

MCF-7, BT474, and MDA-MB453, as well as in MRC5 and normal lymphocytes (Figure 4A).

Finally, we examined by western blot whether L1-*MET* targeting affected MET protein expression, its phosphorylation and the main downstream pathway proteins, namely, AKT and ERK, as a measure of cellular activated signaling.[25] A significant downregulation of MET was detected in EBC1 and GTL16 cancer cells (Figures 4B and S3). In these cells, MET downregulation was associated with reduced levels of phospho-MET (pMET) and phospho-AKT (pAKT) proteins, along with phospho-ERK (pERK) inhibition in EBC1. A mild, not significant, reduction in MET was also observed in A549 and NCI-H1993, while L1-*MET* targeting did not affect MET protein expression in the other cell lines (Figures 4B and S3).

Based on the results of L1-*MET* silencing on cell viability, apoptosis and MET protein expression, the cancer cells were classified as follows: (1) responsive cancer cells, with significant proliferation reduction and increased apoptosis, along with MET/pMET protein knockdown (EBC1 and GTL16) or mild MET decrease (A549); (2) low-responsive cancer cells, with reduced proliferation, but no changes in apoptosis along with mild MET protein decrease (NCI-H1993) or no decrease (MDA-MB231); and (3) non responsive cancer cells, without any

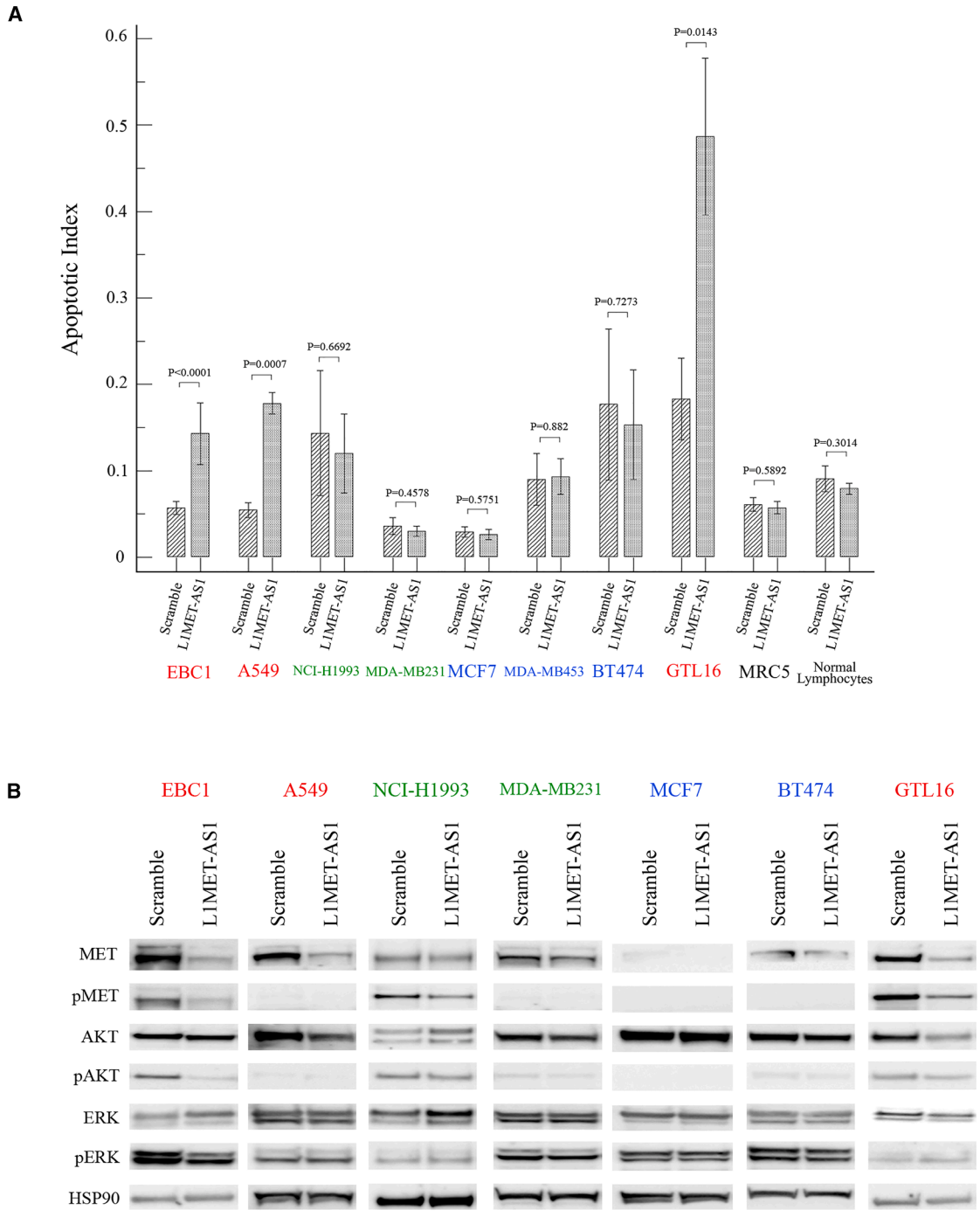

Figure 4. Effects of L1MET_AS1 on the cancer cell panel (EBC-1, A549, NCI-H1993, MDA-MB231, MCF-7, MDA-MB453, BT474, and GTL16) and cell controls (MRC5 and normal lymphocytes) at 24 h after transfection

(A) Bar-plot showing the apoptotic index obtained from cytofluorimetric assay in cancer cell lines and normal cell controls upon transfection of L1-MET_AS1 and scramble gapmers (control); data were obtained by 3 biological replicates ±SD. (B) Western blotting showing the protein expression level of MET/pMET, AKT/pAKT, and ERK/pERK in the cancer cells upon transfection of L1MET_AS1 and scramble gapmers (control); HSP90 was used as protein loading control. Responsive cancer cells, labeled in red; low-responsive cancer cells, labeled in green; non-responsive cancer cells, labeled in blue.

significant effects on proliferation, apoptosis, or MET protein expression (BT474, MDA-MB453, and MCF-7).

Compared effects of the selected L1MET_Gapmers

The second part of our study was aimed at confirming the specificity of the biological effects obtained with the use of L1MET_AS1 and defining the outcomes of the L1-*MET* inhibition on gene expression.

To confirm the previous results, we compared the effects obtained with L1MET_AS1 with those derived from silencing L1-*MET* with the other two *in silico*-selected gapmers, L1MET_AS2 and L1MET_AS3. We focused our analyses on EBC1, A549, MDA-MB231, and MCF-7 cell lines, as they were representative of the different L1-*MET*/*MET* expression and responsiveness to the L1-*MET* inhibition we observed in previous analyses.

Contrary to *in silico* predictions, L1MET_AS2 emerged as the most effective gapmer inducing both a L1-*MET* transcript downregulation and a significant anti-proliferative effect even in the L1MET-AS1 non-responsive MCF-7 cells ($p = 0.028$) (Figures 5A and 5B). In line with the *in silico* predictions, L1MET_AS3 had a limited impact, affecting only the viability of EBC1 cells, which were the most responsive ($p = 0.002$) (Figure 5B). Like the results with L1MET_AS1, the proliferation of control cells (MRC5 and human lymphocytes) remained unaffected by L1-*MET* silencing with either L1MET_AS2 or L1MET_AS3, indicating the absence of any toxic effect (Figure 5B).

In alignment with the cell viability assay, L1MET_AS2 silencing had a pronounced apoptotic effect even in MDA-MB231 and MCF-7 cells ($p = 0.0016$ and $p = 0.0014$) (Figure 5C), while L1MET_AS3 did not affect apoptosis in any of the cancer cells. As expected, MRC5 cells and human lymphocytes showed no changes in apoptotic levels, further confirming the specificity and absence of off-target effects (Figure 5C). Notably, we observed a strong correlation ($p = 0.0002$, rho = 0.881) between the L1-*MET* transcript downregulation and the apoptotic dataset obtained by using all the three selected gapmers.

To evaluate the efficiency of the passive uptake of our gapmers,[26] we tested the anti-proliferative activity of the highly efficient L1MET_AS2 in the most responsive cells, EBC1 and A549, using gymnotic treatment at varying concentrations (5 μM–50 μM). As in the transfection experiments, we used scramble gapmers as negative controls at the same concentrations. We observed a dramatic reduction of the proliferation in EBC1, evident even at the lowest L1MET_AS2 concentration (5 μM). Although to a lesser extent, a significant growth reduction was also observed in A549 cells, correlating with the L1MET_AS2 concentration (Figure S4).

The effects of L1-*MET* silencing on gene expression profile

We explored the impact of L1-*MET* targeting on gene expression profiles using RNA sequencing (RNA-seq) analysis. This analysis was performed on RNA extracted from highly responsive (EBC1 and A549), poorly responsive (MDA-MB231), and weakly/no responsive (MCF-7) cells, at 24 h post-transfection with L1MET_AS1, L1MET_AS2, and scramble gapmers.

To evaluate the broader effects on cancer-related gene sets, we conducted a gene set enrichment analysis (GSEA) (Table S2). Both L1MET_AS1 and L1MET_AS2 treatments consistently triggered positive apoptotic signaling, as evidenced by the upregulation of P53 and tumor necrosis factor alpha (TNF-α) pathways across all cell lines (Figure 6A). This apoptotic activation was typically accompanied by a downregulation of cell cycle-related gene sets, including those associated with the mitotic spindle and G2M checkpoint.[27] Specifically, we observed a uniform downregulation of key cell cycle genes (E2F, MYC, and G2M) and oxidative phosphorylation pathways in all cells following L1-*MET* depletion.

Differential gene expression (DGE) analysis revealed that EBC1 and A549 cells exhibited a substantially higher fraction of deregulated genes compared to MDA-MB-231 and MCF-7 (Figure 6B) (Table S3). Consistent with previous results, *MET* expression was significantly reduced in EBC1 and A549 cells treated with both L1MET_AS1 and L1MET_AS2, MDA-MB231 cells showed a modest downregulation of *MET*, predominantly with L1MET_AS2. In line with the previous results, the already very low *MET* expression in MCF-7 cells was only marginally affected by either treatment (Figure 6B).

Notably, among common cancer-associated genes, we observed a marked decrease in *epidermal growth factor receptor* (*EGFR*) expression in the cancer cells, except in MCF-7, following transfection with L1MET_AS1. Similar results were obtained with L1-MET_AS2 in EBC1 cells (Figures 6C and S5).

L1-*MET* effects on MET and EGFR protein pathways

To validate the gene expression profile results, we examined the status of MET and EGFR proteins, their phosphorylation and the main downstream pathway proteins, in the cancer and not transformed cells transfected with L1MET_AS1, L1MET_AS2, and L1MET_AS3.

In EBC1 cells, which harbor *MET* gene amplification and the *EGFR* activating variant p.L858R, we observed a significant reduction in the expression of both receptors and their corresponding phosphoproteins following treatment with L1MET_AS1 (MET $p = 0.0018$; pMET $p = 0.0256$; EGFR $p = 0.0137$; pEGFR $p = 0.0036$) and L1MET_AS2 (MET $p = 0.0024$; pMET $p = 0.0151$; EGFR $p = 0.0266$; pEGFR $p = 0.0019$). Consistent with these findings, there was a loss of the AKT phosphorylation and a decrease of pERK with both L1MET_AS1 (pAKT $p = 0.0347$; pERK $p = 0.0056$) and L1MET_AS2 (pAKT $p = 0.022$; pERK $p = 0.0011$) (Figures 7A and 7B). A significant reduction of MET, pMET, and downstream pERK were reported even with the less efficient L1MET_AS3 (MET $p = 0.0107$; pMET $p = 0.0464$; pERK $p = 0.0395$) (Figures 7A and 7B).

Conversely, in A549 and MDA-MB231 cells, which are independent of MET and EGFR for their survival, yet express both proteins at

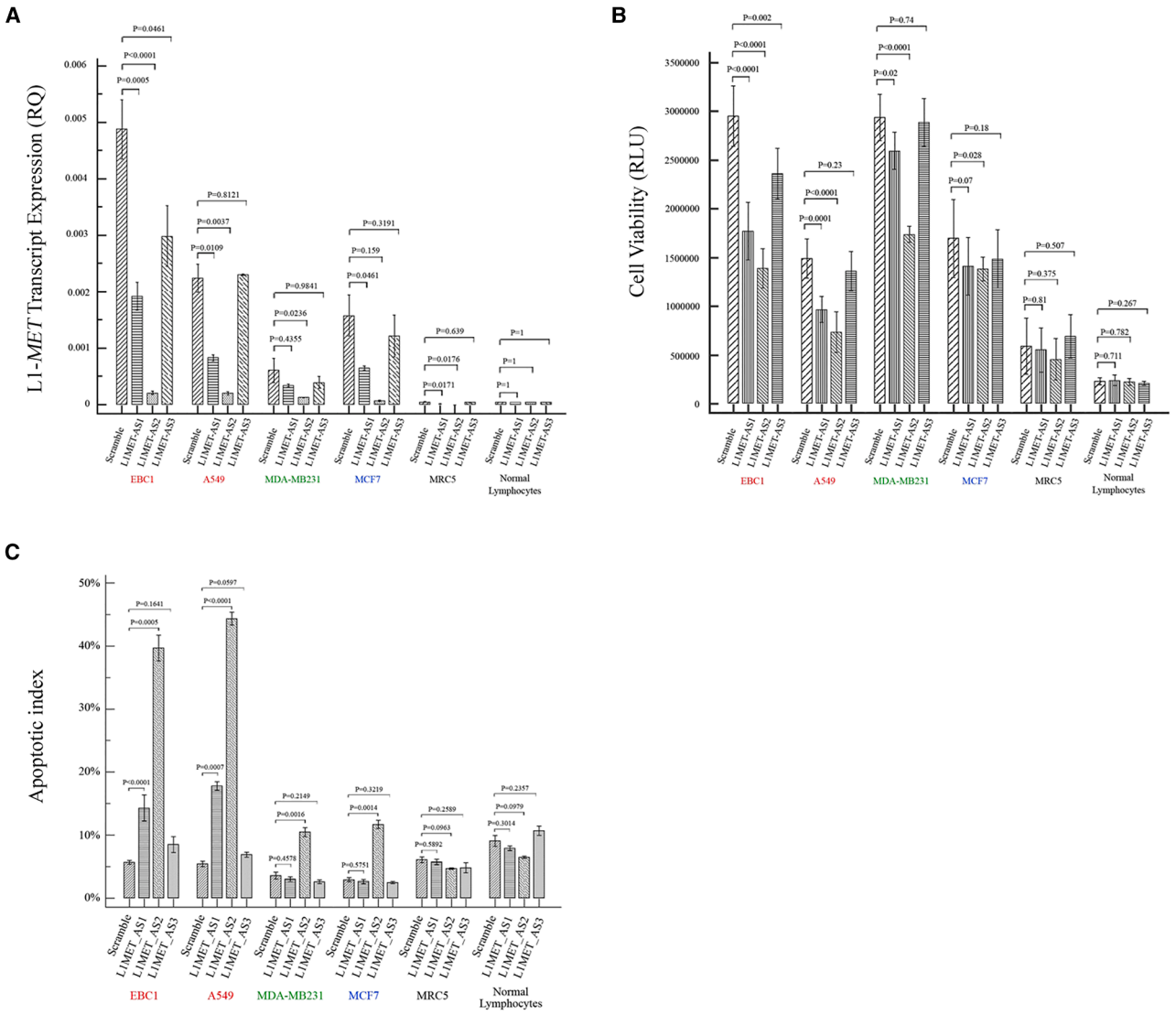

Figure 5. Compared effects of L1MET_AS1/L1MET_AS2/L1MET_AS3 on selected cancer cells (EBC-1, A54, MDA-MB231, and MCF-7) and cell controls (MRC5 and normal lymphocytes) at 24 h after transfection

(A) Bar-plot reporting the expression level of L1-*MET* by real-time qPCR analysis in selected cancer cell lines and cell controls upon transfection of the selected gapmers against L1-*MET* and scramble gapmers (control). (B) Bar-plot showing viability of selected cancer cell lines and cell controls as measured by Cell-titer Glo assay, upon transfection of the selected gapmers against L1-*MET* and scramble gapmers (control). (C) Bar-plot showing the apoptotic index obtained from cytofluorimetric assay in cancer cell lines, MRC5 and normal lymphocytes upon transfection of the selected gapmers against L1-*MET* and scramble gapmers (control). Data are the mean of at least 3 biological replicates ±SD. RQ, relative quantification; RLU, relative light unit. Responsive cancer cells, labeled in red; low-responsive cancer cells, labeled in green; non-responsive cancer cells, labeled in blue.

steady-state levels, no constitutive phosphorylation of the receptors or AKT was detected. However, a strong reduction in MET expression was observed with L1MET_AS2 in both cell lines (A549 $p = 0.0334$; MDA-MB231 $p = 0.0128$), while L1MET_AS1 did not produce a significant difference compared to the control. EGFR expression was also reduced in both the cell lines using either L1MET_AS1 (A549 $p = 0.004$; MDA-MB231 $p = 0.0182$) or L1MET_AS2 (A549 $p = 0.0125$; MDA-MB231 $p = 0.0264$). Unlike in EBC1 cells, no significant reduction of ERK expression or phosphorylation was observed in A549 and MDA-MB231 cells. Moreover, no significant loss of both receptors and their corresponding phospho-proteins was detected after the treatment with L1MET_AS3 (Figures 7A and 7B).

As expected, MCF-7 cells, which do not express MET and EGFR receptors, showed no effects on the expression and phosphorylation status of AKT and ERK following treatment with all the L1MET_

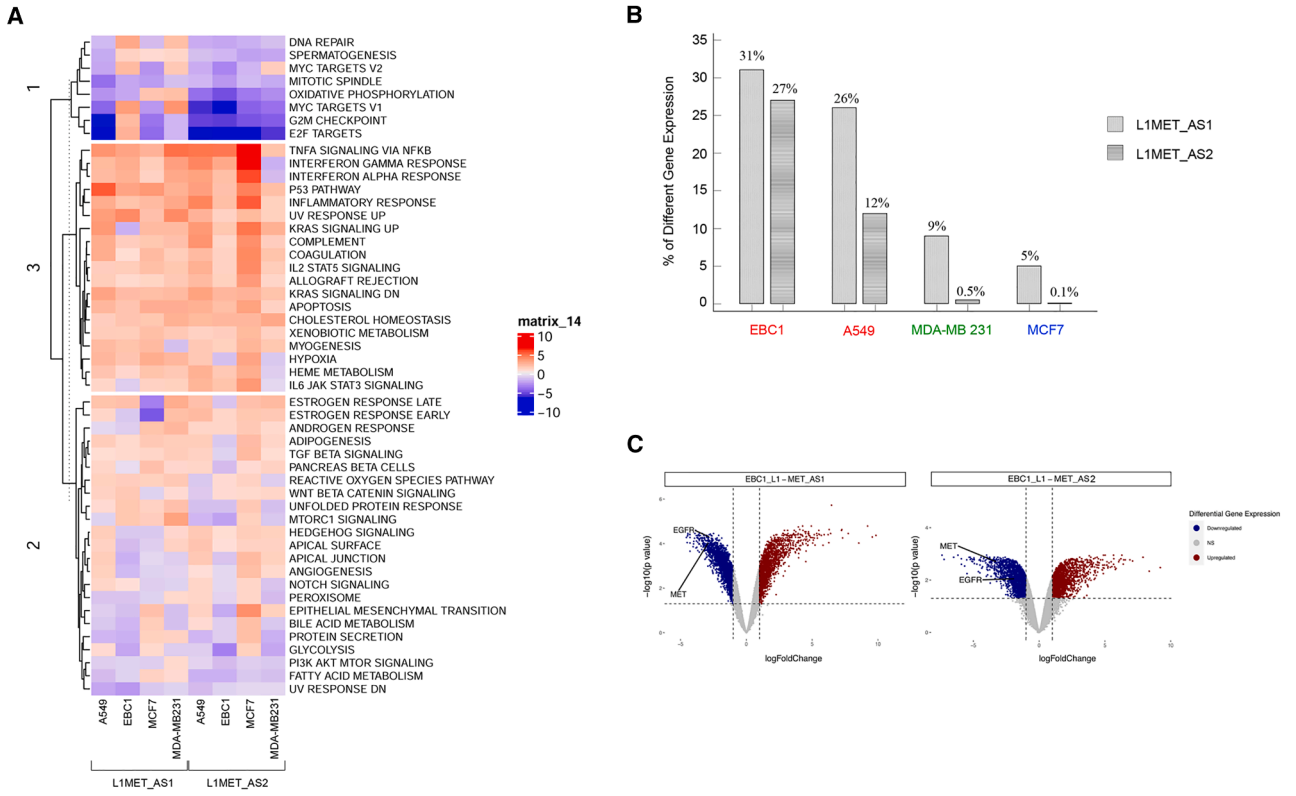

Figure 6. RNA-seq analysis results obtained upon transfection of L1MET_AS1 and L1MET_ AS2 in all the cancer cells

(A) Heatmap reporting the clustering analysis by GSEA, showing the hallmark of cancer gene-sets. (B) Bar-plot showing the differential gene expression (DGE) percentages for each cell line. (C) Volcano plot representing the DGE of the EBC1 cells (L1MET _AS1, top panel; L1MET_AS2, bottom panel): the positions of *MET* and *EGFR* expression are reported. Responsive cancer cells, labeled in red; low-responsive cancer cells, labeled in green; non-responsive cancer cells, labeled in blue.

Gapmers. Similarly, MRC5 fibroblasts, which express very low levels of MET, displayed no significant changes in these markers (Figures 7A and 7B).

DISCUSSION

The L1-*MET* transcript was firstly described by Nigumann et al. in 2002[8]; however, a detailed characterization of its structure and its involvement in aggressive tumor phenotypes has only recently been reported.[13] In this study, we demonstrate that L1-*MET* exerts its transforming effects through the modulation of cell proliferation, apoptosis, and the regulation of key oncogenes. Notably, we have shown that L1-*MET* inhibition significantly impacts the expression of its host gene, *MET*. According to our findings, L1-*MET* transcript is a model of intragenic L1-derived sequences with potential therapeutic applications in activated cancer cells.

Given L1-*MET* location relative to *MET*, we selected gapmers as the most suitable approach to preferentially knockdown the intronic transcript and minimize the effects on *MET* coding sequence. Gapmers are known to efficiently downregulate lncRNA-like transcripts by binding to nuclear and cytoplasmic mRNA, forming a DNA-RNA hybrid that is processed by the RNase-H pathway, ultimately leading to premature transcription termination.[19–21]

To target L1-*MET*, L1MET_Gapmers were carefully selected in a private 76 bp sequence of L1-*MET* transcript, located near the L1-MET promoter (ASP). Moreover, various bioinformatics tools and criteria were used to reduce potential off-target effects.[18] However, due to L1-*MET* position, the selected L1MET_Gapmers could not discriminate between L1-*MET* and nuclear *MET* pre-mRNA. This is an important limitation to distinguish between the effects mediated by L1-*MET* from those directly due to *MET* RNA downregulation. The outcomes of L1MET_AS1 on the L1-*MET*/*MET* mRNA variably expressing cancer cells could suggest a specific targeting of L1-*MET* RNA in one case. Indeed, MDA-MB231 cells, which had *MET* expression, and only very low L1-*MET* level, showed no *MET* mRNA change, but a slight L1-*MET* reduction (14%). Moreover, cells carrying a common *MET* whole gene amplification exhibited a highly variable *MET* mRNA downregulation, which would be unlikely if L1MET_AS1 had played a direct action on *MET* RNA. Nevertheless, these evidences are not conclusive and limited to some of the analyzed cells. Thus, besides the intended L1MET_Gapmer specificity for L1-*MET*, we cannot exclude that the observed effects

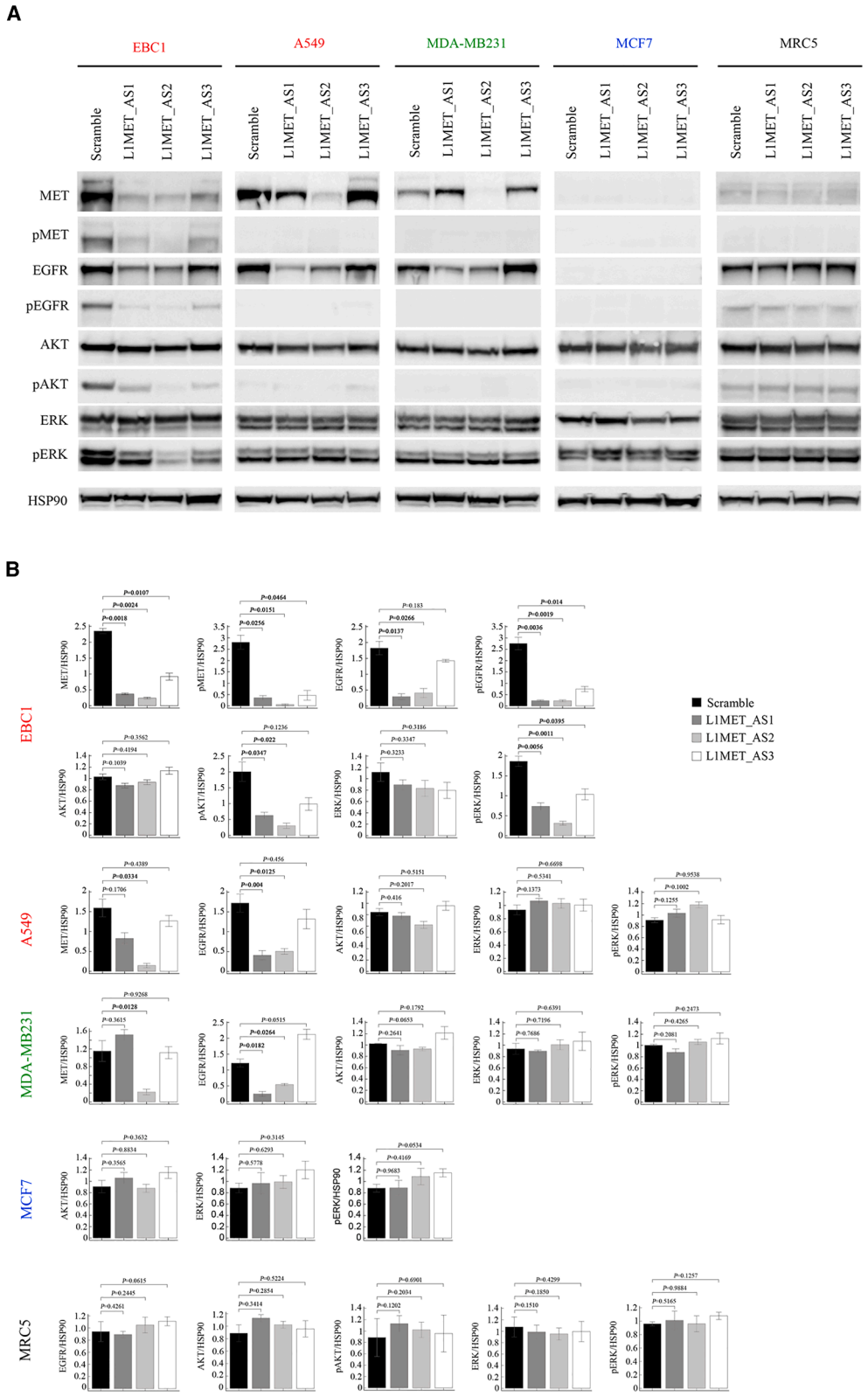

(legend on next page)

on *MET* mRNA are also due to L1MET_Gapmers partially affecting *MET* pre-mRNA nascent transcript.

We identified three gapmers, all of which specifically target the L1-*MET* transcript across the investigated cell lines, albeit with varying effects on cell viability and apoptosis. Ultimately, only two of these gapmers, L1MET_AS1 and L1MET _AS2, were proficient in silencing L1-*MET*, though some discrepancies with *in-silico* predictions were noted. As previously reported,[28] LNA modifications can influence various ASO properties, particularly hybridization efficiency, which can be challenging to predict. This highlights the importance of integrating bioinformatics predictions with experimental validation to optimize the development of effective and specific ASOs.

Previous studies have reported contradictory findings regarding the relationship between L1-*MET* and *MET* expression. While an interdependent relationship has been described in colorectal cancer metastasis and hepatocellular carcinoma,[10,12] a more complex interaction was observed in breast cancer.[13] These discrepancies may be due to tissue-specific factors or the interchangeable use of L1-*MET* methylation and transcript levels to assess L1-*MET* expression. To better understand this interaction, we targeted L1-*MET* expression in a selected panel of cancer cells with varying L1-*MET*/*MET* mRNA levels, representing a spectrum of different conditions, from high to undetectable levels of both transcripts. The panel also included cells lacking detectable L1-*MET* or *MET* expression.

L1-*MET* inhibition induced a decrease in cell viability, even in cells with low L1-*MET* levels. This finding aligns with previous reports on ASO-mediated lncRNA targeting,[21,29,30] suggesting that knocking down even a small amount of L1-*MET* transcript can significantly affect the cancer cell phenotype. The strongest apoptotic effects were observed in cells with the highest level of L1-*MET*, whereas cells with very low L1-*MET* expression, such as MDA-MB231, exhibited increased apoptosis only when L1MET_AS2 was used. As expected from *in silico* predictions, L1MET_AS3 had weaker effects on both L1-*MET* silencing and cell viability. Various factors, such as differences in DNA-RNA binding capabilities,[17] may explain the carrying efficiencies of the L1MET_Gapmers. Notably, in MDA-MB453 cancer cells, as well as in human non-transformed fibroblasts (MRC5) and lymphocytes, which lack detectable L1-*MET* expression, no significant effects were observed, confirming the absence of relevant off-target effects from the selected L1MET_Gapmers.

We detected a variable, but clear downregulation of MET protein in cancer cells with different levels of L1-*MET*/*MET* mRNA. This downregulation was notably associated with decreased expression of downstream proteins in cells with high/intermediate levels of both transcripts. Although the detailed molecular mechanisms underlying the L1-*MET*/*MET* interaction remain partially unclear, these results highlight the importance of *MET* expression. Indeed, the cancer cells most responsive to L1-*MET* silencing included those with *MET* oncogene amplification.

L1-*MET* silencing significantly influenced the gene expression profiles of the analyzed cells, particularly the lung cancer cells (EBC1 and A549). In addition to the upregulation of genes related to P53 and downregulation of cell-cycle genes, including those controlling the G2/M phase checkpoint and mitotic spindle formation,[27] we observed downregulation of genes associated with the G1-S phase transition (EF2 pathway) and DNA repair. These findings corroborated the effects detected in cell viability and cytofluorimetric analysis.

Gene expression profile data supported a direct or indirect involvement of L1-*MET* in the transcriptional regulation of hosting *MET*, on chromosome 7q31.2, but also of *EGFR*, located on 7p11.2. Regarding *MET* transcription, L1-*MET*, which retains the same *MET* 3′UTR and contains *MET*-specific miRNA response elements[31] might act as competing endogenous RNA.[32] Alternatively, L1 activation in *MET* intron 2 might exert a master chromosomal effect and regulates *MET* promoter/enhancer utilization through L1-*MET*. As far as *EGFR* regulation, lncRNA mechanisms regulating the expression of unlinked genes might be involved, including interaction with promoters and enhancers, chromatin state modulation or interchromosomal interactions.[33] Accordingly, Marasca et al. (2022)[34] showed that L1-containing transcripts can influence the transcription of genes in which they are embedded and act *in trans*, modulating the expression of distant genes.

The protein expression data for EGFR confirmed the transcription results, showing a clear downregulation of EGFR protein following L1-*MET* silencing in EGFR-expressing cancer cells. This effect was independent of MET or EGFR phosphorylation status, as demonstrated by our panel of cells, which included MET- and EGFR-phosphorylated cells (EBC1) as well as cells expressing unphosphorylated MET and EGFR protein (A549 and MDA-MB231). In EBC1 cells, the downregulation of MET and EGFR proteins also leads to a reduction in the corresponding phospho-proteins, resulting in the loss of AKT and ERK phosphorylation, mimicking the effects obtained by MET inhibitors.[35–37]

There is a pressing need for broad-spectrum drugs that can overcome the limitations of standard anti-cancer therapies. Currently, ASOs represent a promising approach to therapeutic lncRNA treatment, with several mRNA targeting ASOs already approved by Food

Figure 7. Protein expression results upon transfection of L1MET_AS1, L1MET_AS2, and L1MET_AS3 in cancer and non-transformed (MRC5) cells

(A) Western blotting showing the protein expression level in all the cells tested; HSP90 was used as protein loading control. (B) Bar-plot reporting the quantification of band intensity of MET/pMET, EGFR/pEGFR, AKT/pAKT normalized on the intensity of HSP90 loading control; data were obtained by 3 biological replicates ±SD. Responsive cancer cells, labeled in red; low-responsive cancer cells, labeled in green; non-responsive cancer cells, labeled in blue.

and Drug Administration (FDA) and European Medicines Agency (EMA), and others in clinical trials or under development.[38,39] However, there are still important limitations to consider in the ASO-based strategies, such as the risk of developing specific hepatotoxicity, kidney toxicity, and hypersensitivity reactions.[40] Moreover, the precise molecular and biochemical mechanisms of these events are still unclear.[41] Gapmers seem to be particularly promising due to the low immunogenicity and sequence-dependent toxicity, making them an encouraging option in the context of the ncRNA-based cancer therapies.[42,43] Nonetheless, in our hands, the use of L1MET_-Gapmers resulted in the interferon (IFN)-γ upregulation, which can represent another important side effect to be considered in the ASO-therapy application. Several studies are presently focused on clarifying IFN-γ-dependent pro- and anti-tumorigenic effects to improve our understanding of the cancer context in which ASO-therapy can be successfully applied.[44] Delivery of ASO drugs to specific tissues and cellular uptake poses another great challenges. The improvement of ASO modification, together with the development of different types of nano-drug delivery vehicles, is expected to strongly ameliorate the ASO application in the next future.[45]

The high selectivity of L1MET_Gapmers for tumor cells relies on the absence of L1-*MET* transcript expression in normal cells or tissues, as well as in its specific activation by hypomethylation[2–5]—a common alteration acquired during the early stages of transformation in various tissues. Accordingly, several types of cancer cells, including lung, breast, and gastric tumor cells, were affected by L1-*MET* silencing. Although the best results were obtained in cells with activated *MET* and *EGFR* genes, significant effects were also observed in tumor cells with steady-state expression of these oncoproteins and/or addiction to other oncogenes.

Further robust *in vivo* validations and broader tumor spectrum screenings are necessary to establish the use of L1MET_Gapmers as a viable clinical tool. Pre-clinical studies in organoids and patient-derived-cancer (PDX) models obtained from L1-*MET* expressing tumors will be helpful to verify the L1MET_Gapmers efficacy and proper administration *in vivo*.

In conclusion, the results presented here support L1-*MET* silencing as a promising therapeutic approach, capable of overcoming the disadvantages of conventional targeted therapies, such as resistance to tyrosine kinase inhibitor treatments, particularly in *MET*- and *EGFR*-activated tumors.

MATERIALS AND METHODS

Cancer cell lines

MDA-MB231 (RRID:CVCL_0062) and MCF-7 (RRID:CVCL_0031) cell lines were obtained from NCI-60, EBC1 (RRID:CVCL_2891) from the Health Science Research Resources Bank, A549 (RRID:CVCL_0023), NCI-H1993 (RRID:CVCL_1512) and MRC5 (RRID:CVCL_0440) from the American Type Culture Collection, BT474 (RRID:CVCL_0179) from Leibniz Institute (DSMZ), MDA-MB453 (RRID:CVCL_0418) from the IRCCS Ospedale Policlinico San Martino cell bank (ICLC), and GTL16 (RRID:CVCL_7668) from Candiolo Cancer Institute cell bank. The human lymphocytes belonged to a healthy donor who gave the consent for the experiments.

EBC1, NCI-H1993, A549, and GTL16 cells were grown in RPMI with 10% FBS; MDA-MB231 in high-glucose DMEM with 10% FBS; MCF-7 cells in high-glucose DMEM with 10% FBS supplemented with 10 μg/mL insulin; BT474 in RPMI with 20% FBS supplemented with 10 μg/mL insulin; MDA-MB453 in L-15 with 10% FBS incubated without CO2; MRC5 in MEM with 10% FBS. All cell lines were authenticated using short tandem repeat profiling within the last three years (PowerPlex 16 HS System, Promega, Madison, WI). All experiments were performed with mycoplasma-free cells. To this purpose, cells were periodically tested for mycoplasma contamination using the Venor GM kit (Minerva Biolabs, Berlin, Germany). Normal lymphocytes from one healthy donor were obtained from peripheral blood using the lymphocyte cell separation media (Cedarlane, Burlington, Canada), and grown in RPMI with 10% FBS.

To characterize the mutational profile of the cells, DNA was extracted using the QIAamp DNA kit (Qiagen, Hilden, Germany). Mutational analysis was performed by the mass spectrometry matrix-assisted laser desorption ionization time of flight method with the MassARRAY System (Agena Bioscience, Hamburg, Germany), using the Myriapod Lung status panel (Diatech Pharmacogenetics, Jesi, Italy) that allows to search for hotspot mutations in the following genes: *EGFR*, *KRAS*, *BRAF*, *NRAS*, *PIK3CA*, *ALK*, *ERBB2*, *DDR2*, *RET*, and *MAP2K1*. Experiments were performed following the manufacturer's instructions. The *MET* gene amplification was evaluated by FISH in interphase nuclei using the ZytoLight SPEC MET/CEN 7 Dual Color Probe (ZytoVision, Bremerhaven, Germany), according to the manufacturer's instructions. *MET* FISH-positive criteria included 5 or more *MET* signals per cell, as reported in Cappuzzo et al. (2009).[46]

Antisense oligonucleotide selection

According to the reported criteria in https://blast.ncbi.nlm.nih.gov/Blast.cgi, a specific 76 bp sequence of the L1-*MET* transcript was selected and investigated by five designer tools (BLOCK-iT RNAi Designer; siRNA wizard software; I-score designer; siRNA at whitehead; siDirect version 2.0) to identify the best L1-*MET* targeting ASOs. This *in silico* analysis led to pinpoint a set of 11 ASO-accessible sequences (Table 1). Qualitative features of the ASOs (e.g., structural, chemical, and sequence composition) depend on the accessibility of the target mRNA[18] (https://www.ensembl.org/Homo_sapiens/Tools/Blast). To this purpose, sFOLD web tool (https://sfold.wadsworth.org) was used to check the secondary structures of the 11 identified ASOs and the folding of the target regions in the L1-MET mRNA.

After these screenings, 3 out of the 11 ASOs were chosen and used by Exiqon (Qiagen, Hilden, Germany) to synthesize the corresponding gapmers (namely, L1MET_AS1, L1MET_AS2, and L1MET_AS3) which were LNA modified by connecting the ribose ring by a

methylene bridge between the 2′-O and 4′-C atoms. The LNA content of the three oligonucleotides was checked by the manufacturer to achieve good mismatch discrimination and high binding specificity, while avoiding unacceptable secondary structure and self-complementarity.[18]

RNA extraction and quantitative real-time PCR analysis

RNA was extracted from cell lines and lymphocytes using the Maxwell RSC miRNA tissue kit (Promega), following the manufacturer's instruction, quantified using the DeNovix spectrophotometer (DeNovix, Wilmington, Delaware), and checked for a RIN >8. One μg RNA was then reverse transcribed in a mix containing oligo(dT) and random hexamers, using the Reverse Transcription System (Promega). To investigate the expression of L1-*MET* and *MET*, real-time qPCR was performed using a common reverse primer on *MET* exon 3 with a forward primer on the L1-ORF0 region and on exon 2, for L1-*MET* and *MET*, respectively. Their localization is described in Figures 1 and S1, whereas their sequences and PCR condition are reported in Table S1. Relative expression quantification (RQ) was calculated according to the following formula reported here[47] using GAPDH as endogenous control: RQ = 2−(ΔCt) where ΔCt = (Ct L1-MET − Ct GAPDH).

Transient transfections and gymnosis experiments

Cultured cells were transiently transfected with the different gapmers using Lipofectamine RNAiMAX (Thermo Fisher Scientific, Waltham, Massachusetts), according to the manufacturer's protocol. As a control, a specific gapmers for *MALAT1* gene and scramble gapmers were also transfected. The day of the transfection, 6×10^5 cells/dish were seeded in a 10 cm tissue culture dish with the appropriate growing medium, in the presence of the transfection mix. The efficacy of the silencing protocol was confirmed by the decreasing gene expression of the control gene *MALAT1* in all cells. To evaluate the transfection efficiency and the gapmers toxicity, L1-*MET* was tested by real-time qPCR for different gapmers concentrations (5 nM, 10 nM, and 25 nM) and time (24 h and 48 h after transfection). No evident toxicity was detected. We choose 25 nM and 24 h as the optimal conditions to carry out the subsequent analyses.

To test the ability of the gapmers to enter the cell without a transfection reagent, a gymnosis delivery was performed on EBC1 and A549 cell lines, as previously reported.[26] Briefly, 3×10^3 cells/well were seeded in a 96-well plate with the appropriate growing medium. The day after plating, the gapmers dissolved in PBS were added to the cell culture at four different concentrations: 5 μM, 10 μM, 25 μM, and 50 μM. Scramble gapmers at the same concentrations were used as negative controls. After 6 days of incubation cells were fixed with 3% of paraformaldehyde and stained with 1% crystal violet-methanol solution (Sigma Aldrich). Crystal violet was solubilized with 10% of acetic acid and the absorbance was quantified at 595 nm.

Cell viability and apoptosis assay

Cell viability was evaluated using the CellTiter-Glo kit (Promega). Transfections were performed in a 6-fold experiment with 25 nM of each gapmers, in a 96-well plate in which 3,000 cells/well were seeded. Luminescence was acquired after 24 h from the transfection using the Tecan Spark 10M instrument (TECAN, Männedorf, Switzerland).

Apoptosis assay was carried out by cytofluorimeter using propidium iodide and annexin V APC-conjugated (Thermo Fisher Scientific). Cells were transfected in 10-cm plates as described previously. After 24 h from transfection, cells were detached using trypsin-EDTA solution (1×, Sigma-Aldrich, St. Louis, Missouri), washed three times with PBS, and incubated for 15 min at 4°C with annexin V APC-conjugated and propidium iodide in binding buffer solution (0.5 M HEPES, 0.15 M NaCl, and 0.005 M $CaCl_2$). Acquisition was performed on CyAn cytometer (Beckman Coulter, Brea, California) using the Summit v4.3 software to analyze the data (Dako Colorado, INC.). Apoptotic index was expressed as the percentage of apoptotic cells and calculated using the formula: (number of early apoptotic cells + number of late apoptotic cells) / total detected cells.

RNA-seq analysis

RNA-seq analysis was performed after the L1-*MET* antisense oligo transfections of the cancer cells (A549, EBC1, MDA-MB231, and MCF-7). In detail, the RNA purified from the cells transfected with the L1MET_AS1, L1MET_AS2, or with the scramble gapmers was analyzed in three independent replicating experiments. All the library preparation was performed using the TruSeq stranded mRNA kit (Illumina, San Diego, California), starting from 1 μg of total RNA with a RIN >8. Briefly, after the purification of the poly-A RNA (e.g., mRNA) using the poly-T oligo attached magnetic beads, the cDNA was synthetized, end-repaired and adenylated to the 3′ end to allow the ligation of the indexed adapters. The pooled libraries were then loaded on Illumina NextSeq 500/550 instruments to a final concentration of 1.1 pM for single-end 75 bp sequencing. Passing filters reads were aligned to GRCh38 primary assembly genome, downloaded from GENCODE (version 29)[48] using STAR (version 2.5.4a with custom parameters – outFilterMultimapNmax 10 – outFilterMultimapScoreRange 1 – outFilterMismatchNmax 999 – outFilterMismatchNoverLmax 0.08).[49] For gene expression quantification, read was assigned to exons using subread featureCounts v1.6.3, discarding multi mapping reads and ambiguous reads and summarizing over gene names. As reference, transcript annotation GENCODE basic annotation (version 29) was used, complemented with custom tracks of L1-*MET* transcripts described in Miglio et al.[13] The same complemented transcript annotation was used to build the STAR index. The sequence coverage and quality data are reported in Table S4.

Gene expression counts were next analyzed using the edgeR package (https://doi.org/10.1093/bioinformatics/btp616). After the filtration of low-expressed genes (1 count per million [CPM] in less than 9 samples), normalization factors were calculated using the trimmed-mean of M-values (TMM) method (implemented in the calcNormFactors function) and CPM was obtained using normalized library sizes. Differential expression analysis was carried out independently for each cell line and each ASO by fitting genewise

GLMs to the read counts blocking for replicates (formula ~0+silencing+replicate). Quasi-likelihood F-test was used to compare gene expression in treated and untreated cells computing log fold changes and p values. Multiplicity correction is performed by applying the Benjamini-Hochberg method on the p values to control the false discovery rate. Processed sequencing data are reported in Tables S2 and S3.

Protein extraction and western blot analysis

Proteins were extracted 24 h after transfection from all cells using hot lysis protocol.[50] The lysate was collected in a 1.5 mL tube and incubated at 95°C for 15 min. After sonication, proteins were quantified using the spectrophotometer with the Pierce BCA Protein Assay kit (Thermo Fisher Scientific). Fifty ng of protein were separated by SDS-polyacrylamide gel electrophoresis (Bolt 4%–12% Bis-Tris Plus gel) (Thermo Fisher Scientific) and blotted on Trans-Blot Turbo nitrocellulose membranes (Bio-Rad, Hercules, California). Membranes were blocked for 45 min with TBS-T containing 10% BSA or 5% nonfat dry milk, depending on the antibodies used. Membranes were then incubated overnight at 4°C with the following antibodies: anti-AKT (2972), anti-p44/42 MAPK (9102) anti-phospho-AKT Ser473 (9271), anti-phospho-p44/42 MAPK Thr202/Tyr204 (9101), anti-phospho-EGFR Tyr1068 (3777), anti-phospho-MET Tyr1234/1235 (3077) (Cell Signaling Technology, Danvers, Massachusetts), anti-MET (DL21) homemade, and anti-EGFR (1005 sc-03) (Santa Cruz, Santa Cruz, California). All the primary antibodies were diluted 1:1,000. Appropriate HRP-conjugated secondary antibodies (1:10,000 – Jackson ImmunoResearch Laboratories, Inc.) were used for detection with chemiluminescence using the Clarity Western ECL Substrate (Bio-Rad). Image acquisition and analysis was performed using the ImageLab software (Bio-Rad).

Statistical analysis

Data analysis was carried out with MedCalc statistical software 13.0.6 (MedCalc Software bvba, Ostend, Belgium) and R software (R Foundation for Statistical Computing, Vienna, Austria). Student's t-distribution and standard deviation (SD) were used to determine differences between groups of replicated samples. p values were determined with the Mann-Whitney and Kruskal-Wallis tests and $p < 0.05$ were considered statistically significant. Correlation test was performed using the Spearman test, with $p < 0.05$ considered statistically significant. GSEA was performed using logFC for each comparison as pre-rank scores for gene, normalized enrichment scores were computed using 1000-fold permutation test and clustered using Euclidean distance and complete linkage (Table S2).

DATA AVAILABILITY

All data are included in the manuscript and in the supplemental information; processed sequencing data are available at https://www.ncbi.nlm.nih.gov/geo/query/acc.cgi?acc=GSE220194. Reviewers can use the following code to access the data: gvajkocgfjaxzmt.

ACKNOWLEDGMENTS

The authors thank Silvia Benvenuti, Paolo Comoglio, and Giulio Ferrero for their helpful discussions and Jessica Pantaleo, Paola Bernabei, and Raffaella Albano for their technical support. This research was funded by FPRC 5x1000 Ministero Salute 2020 PRO-ACTIVE; FPRC 5x1000 Ministero Salute 2021 PTRC Intra-2020; Italian Ministry of Health, Ricerca Corrente 2024–2025. E.B. was the recipient of a Ph.D. fellowship under the funding of Dipartimenti di Eccellenza 2018–2022 (project no. 521 D15D18000410001). E.M. was supported by a CDP Special Fellow Award from the Leukemia and Lymphoma Society and an FPRC 5x1000 Ministero della Salute 2021 (EmaGen-LongMynd). In memory of Laura Annaratone.

AUTHOR CONTRIBUTIONS

Conceptualization, U.M., E.B., and T.V.; methodology, E.B., U.M., V.M., M.D.B., L.L., E. M., and T.V.; analysis, U.M., E.B., D.A., and M.M.; bioinformatics analysis, I.M.; data curation, U.M., E.B., A.S., and T.V.; supervision, T.V. and A.S.; writing – original draft, U.M., E.B., and T.V.; review and editing, V.M., L.L., M.D.B., E.M., J.M.H., and T.V. All authors have read and agreed to the submitted version.

DECLARATION OF INTERESTS

The antisense sequences (ASOs) to target L1-*MET* were patented by T.V. under license no. IT201900021327A1.

SUPPLEMENTAL INFORMATION

Supplemental information can be found online at https://doi.org/10.1016/j.omtn.2025.102529.

REFERENCES

1. Wanichnopparat, W., Suwanwongse, K., Pin-On, P., Aporntewan, C., and Mutirangura, A. (2013). Genes associated with the cis-regulatory functions of intragenic LINE-1 elements. BMC Genom. *14*, 205.
2. Kazazian, H.H., Jr., and Moran, J.V. (2017). Mobile DNA in Health and Disease. N. Engl. J. Med. *377*, 361–370.
3. Mueller, C., Aschacher, T., Wolf, B., and Bergmann, M. (2018). A role of LINE-1 in telomere regulation. Front. Biosci. *23*, 1310–1319.
4. Ponomaryova, A.A., Rykova, E.Y., Gervas, P.A., Cherdyntseva, N.V., Mamedov, I.Z., and Azhikina, T.L. (2020). Aberrant Methylation of LINE-1 Transposable Elements: A Search for Cancer Biomarkers. Cells *9*, 2017.
5. Speek, M. (2001). Antisense promoter of human L1 retrotransposon drives transcription of adjacent cellular genes. Mol. Cell Biol. *21*, 1973–1985.
6. Criscione, S.W., Theodosakis, N., Micevic, G., Cornish, T.C., Burns, K.H., Neretti, N., and Rodić, N. (2016). Genome-wide characterization of human L1 antisense promoter-driven transcripts. BMC Genom. *17*, 463.
7. Matlik, K., Redik, K., and Speek, M. (2006). L1 antisense promoter drives tissue-specific transcription of human genes. J. Biomed. Biotechnol. *2006*, 71753.
8. Nigumann, P., Redik, K., Mätlik, K., and Speek, M. (2002). Many human genes are transcribed from the antisense promoter of L1 retrotransposon. Genomics *79*, 628–634.
9. Wolff, E.M., Byun, H.M., Han, H.F., Sharma, S., Nichols, P.W., Siegmund, K.D., Yang, A.S., Jones, P.A., and Liang, G. (2010). Hypomethylation of a LINE-1 promoter activates an alternate transcript of the MET oncogene in bladders with cancer. PLoS Genet. *6*, e1000917.
10. Zhu, C., Utsunomiya, T., Ikemoto, T., Yamada, S., Morine, Y., Imura, S., Arakawa, Y., Takasu, C., Ishikawa, D., Imoto, I., and Shimada, M. (2014). Hypomethylation of long interspersed nuclear element-1 (LINE-1) is associated with poor prognosis via activation of c-MET in hepatocellular carcinoma. Ann. Surg Oncol. *21*, S729–S735.
11. Furlan, D., Trapani, D., Berrino, E., Debernardi, C., Panero, M., Libera, L., Sahnane, N., Riva, C., Tibiletti, M.G., Sessa, F., et al. (2017). Oxidative DNA damage induces hypomethylation in a compromised base excision repair colorectal tumourigenesis. Br. J. Cancer *116*, 793–801.
12. Hur, K., Cejas, P., Feliu, J., Moreno-Rubio, J., Burgos, E., Boland, C.R., and Goel, A. (2014). Hypomethylation of long interspersed nuclear element-1 (LINE-1) leads to activation of proto-oncogenes in human colorectal cancer metastasis. Gut *63*, 635–646.
13. Miglio, U., Berrino, E., Panero, M., Ferrero, G., Coscujuela Tarrero, L., Miano, V., Dell'Aglio, C., Sarotto, I., Annaratone, L., Marchiò, C., et al. (2018). The expression

of LINE1-MET chimeric transcript identifies a subgroup of aggressive breast cancers. Int. J. Cancer *143*, 2838–2848.

14. Comoglio, P.M., Trusolino, L., and Boccaccio, C. (2018). Known and novel roles of the MET oncogene in cancer: a coherent approach to targeted therapy. Nat. Rev. Cancer *18*, 341–358.
15. Fatica, A., and Bozzoni, I. (2014). Long non-coding RNAs: new players in cell differentiation and development. Nat. Rev. Genet. *15*, 7–21.
16. Weber, B., Kimhi, S., Howard, G., Eden, A., and Lyko, F. (2010). Demethylation of a LINE-1 antisense promoter in the cMet locus impairs Met signalling through induction of illegitimate transcription. Oncogene *29*, 5775–5784.
17. Shen, X., and Corey, D.R. (2018). Chemistry, mechanism and clinical status of antisense oligonucleotides and duplex RNAs. Nucleic Acids Res. *46*, 1584–1600.
18. Bo, X., Lou, S., Sun, D., Shu, W., Yang, J., and Wang, S. (2006). Selection of antisense oligonucleotides based on multiple predicted target mRNA structures. BMC Bioinf. *7*, 122.
19. Lai, F., Damle, S.S., Ling, K.K., and Rigo, F. (2020). Directed RNase H Cleavage of Nascent Transcripts Causes Transcription Termination. Mol. Cell *77*, 1032–1043.e4.
20. Lee, J.S., and Mendell, J.T. (2020). Antisense-Mediated Transcript Knockdown Triggers Premature Transcription Termination. Mol. Cell *77*, 1044–1054.e3.
21. Zong, X., Huang, L., Tripathi, V., Peralta, R., Freier, S.M., Guo, S., and Prasanth, K.V. (2015). Knockdown of nuclear-retained long noncoding RNAs using modified DNA antisense oligonucleotides. Methods Mol. Biol. *1262*, 321–331.
22. Hagedorn, P.H., Persson, R., Funder, E.D., Albæk, N., Diemer, S.L., Hansen, D.J., Møller, M.R., Papargyri, N., Christiansen, H., Hansen, B.R., et al. (2018). Locked nucleic acid: modality, diversity, and drug discovery. Drug Discov. Today *23*, 101–114.
23. Ponzetto, C., Giordano, S., Peverali, F., Della Valle, G., Abate, M.L., Vaula, G., and Comoglio, P.M. (1991). c-met is amplified but not mutated in a cell line with an activated met tyrosine kinase. Oncogene *6*, 553–559.
24. Lutterbach, B., Zeng, Q., Davis, L.J., Hatch, H., Hang, G., Kohl, N.E., Gibbs, J.B., and Pan, B.S. (2007). Lung cancer cell lines harboring MET gene amplification are dependent on Met for growth and survival. Cancer Res. 67:2081-8 *15*, 3987. Erratum in: Cancer Res (2007).
25. Ardito, F., Giuliani, M., Perrone, D., Troiano, G., and Lo Muzio, L. (2017). The crucial role of protein phosphorylation in cell signaling and its use as targeted therapy (Review). Int. J. Mol. Med. *40*, 271–280.
26. Stein, C.A., Hansen, J.B., Lai, J., Wu, S., Voskresenskiy, A., Høg, A., Worm, J., Hedtjärn, M., Souleimanian, N., Miller, P., et al. (2010). Efficient gene silencing by delivery of locked nucleic acid antisense oligonucleotides, unassisted by transfection reagents. Nucleic Acids Res. *38*, e3.
27. Chen, J. (2016). The Cell-Cycle Arrest and Apoptotic Functions of p53 in Tumor Initiation and Progression. Cold Spring Harb Perspect *6*, a026104.
28. Watt, A.T., Swayze, G., Swayze, E.E., and Freier, S.M. (2020). Likelihood of Nonspecific Activity of Gapmer Antisense Oligonucleotides Is Associated with Relative Hybridization Free Energy. Nucleic Acid Ther. *30*, 215–228.
29. Lennox, A.L., Hoye, M.L., Jiang, R., Johnson-Kerner, B.L., Suit, L.A., Venkataramanan, S., Sheehan, C.J., Alsina, F.C., Fregeau, B., Aldinger, K.A., et al. (2020). Pathogenic DDX3X Mutations Impair RNA Metabolism and Neurogenesis during Fetal Cortical Development. Neuron *106*, 404–420.e8.
30. Taiana, E., Gallo Cantafio, M.E., Favasuli, V.K., Bandini, C., Viglietto, G., Piva, R., Neri, A., and Amodio, N. (2021). Genomic Instability in Multiple Myeloma: A "Non-Coding RNA" Perspective. Cancers (Basel) *13*, 2127.
31. Yan, D., Dong, X.D.E., Chen, X., Wang, L., Lu, C., Wang, J., Qu, J., and Tu, L. (2009). MicroRNA-1/206 targets c-Met and inhibits rhabdomyosarcoma development. J. Biol. Chem. *284*, 29596–29604.
32. Poliseno, L., Salmena, L., Zhang, J., Carver, B., Haveman, W.J., and Pandolfi, P.P. (2010). A coding-independent function of gene and pseudogene mRNAs regulates tumour biology. Nature *465*, 1033–1038.
33. Kopp, F., and Mendell, J.T. (2018). Functional Classification and Experimental Dissection of Long Noncoding RNAs. Cell *172*, 393–407.
34. Marasca, F., Sinha, S., Vadalà, R., Polimeni, B., Ranzani, V., Paraboschi, E.M., Burattin, F.V., Ghilotti, M., Crosti, M., Negri, M.L., et al. (2022). LINE1 are spliced in non-canonical transcript variants to regulate T cell quiescence and exhaustion. Nat. Genet. *54*, 180–193.
35. Tanizaki, J., Okamoto, I., Okamoto, K., Takezawa, K., Kuwata, K., Yamaguchi, H., and Nakagawa, K. (2011). MET tyrosine kinase inhibitor crizotinib (PF-02341066) shows differential antitumor effects in non-small cell lung cancer according to MET alterations. J. Thorac. Oncol. *6*, 1624–1631.
36. Tsien, C.I., Nyati, M.K., Ahsan, A., Ramanand, S.G., Chepeha, D.B., Worden, F.P., Helman, J.I., D'Silva, N., Bradford, C.R., Wolf, G.T., et al. (2013). Effect of erlotinib on epidermal growth factor receptor and downstream signaling in oral cavity squamous cell carcinoma. Head Neck *35*, 1323–1330.
37. Martin, V., Corso, S., Comoglio, P.M., and Giordano, S. (2014). Increase of MET gene copy number confers resistance to a monovalent MET antibody and establishes drug dependence. Mol. Oncol. *8*, 1561–1574.
38. Di Fusco, D., Dinallo, V., Marafini, I., Figliuzzi, M.M., Romano, B., and Monteleone, G. (2019). Antisense Oligonucleotide: Basic Concepts and Therapeutic Application in Inflammatory Bowel Disease. Front. Pharmacol. *10*, 305.
39. Zhang, Y., Qu, Z., Kraft, P., Shi, V., Qu, Z., Liao, B., Bandaru, R., Wu, Y., Greenberger, L.M., Horak, I.D., et al. (2011). Down-modulation of cancer targets using locked nucleic acid (LNA)-based antisense oligonucleotides without transfection. Gene Ther. *18*, 326–333.
40. Lauffer, M.C., van Roon-Mom, W., and Aartsma-Rus, A. (2024). Collaborative. Possibilities and limitations of antisense oligonucleotide therapies for the treatment of monogenic disorders. Commun. Med. *4*, 6.
41. Alhamadani, F., Zhang, K., Parikh, R., Wu, H., Rasmussen, T.P., Bahal, R., Zhong, X. B., and Manautou, J.E. (2022). Adverse Drug Reactions and Toxicity of the Food and Drug Administration-Approved Antisense Oligonucleotide Drugs. Drug Metab. Dispos. *50*, 879–887.
42. Morelli, E., Biamonte, L., Federico, C., Amodio, N., Di Martino, M.T., Gallo Cantafio, M.E., Manzoni, M., Scionti, F., Samur, M.K., Gullà, A., et al. (2018). Therapeutic vulnerability of multiple myeloma to MIR17PTi, a first-in-class inhibitor of pri-miR-17-92. Blood *132*, 1050–1063.
43. Adewunmi, O., Shen, Y., Zhang, X.H.F., and Rosen, J.M. (2023). Targeted Inhibition of lncRNA Malat1 Alters the Tumor Immune Microenvironment in Preclinical Syngeneic Mouse Models of Triple-Negative Breast Cancer. Cancer Immunol. Res. *11*, 1462–1479.
44. Castro, F., Cardoso, A.P., Gonçalves, R.M., Serre, K., and Oliveira, M.J. (2018). Interferon-Gamma at the Crossroads of Tumor Immune Surveillance or Evasion. Front. Immunol. *9*, 847.
45. Gagliardi, M., and Ashizawa, A.T. (2021). The Challenges and Strategies of Antisense Oligonucleotide Drug Delivery. Biomedicines *9*, 433.
46. Cappuzzo, F., Jänne, P.A., Skokan, M., Finocchiaro, G., Rossi, E., Ligorio, C., Zucali, P.A., Terracciano, L., Toschi, L., Roncalli, M., et al. (2009). MET increased gene copy number and primary resistance to gefitinib therapy in non–small-cell lung cancer patients. Ann. Oncol. *20*, 298–304.
47. Berrino, E., Miglio, U., Bellomo, S.E., Debernardi, C., Bragoni, A., Petrelli, A., Cascardi, E., Giordano, S., Montemurro, F., Marchiò, C., et al. (2022). The Tumor-Specific Expression of L1 Retrotransposons Independently Correlates with Time to Relapse in Hormone-Negative Breast Cancer Patients. Cells *11*, 1944.
48. Liao, Y., Smyth, G.K., and Shi, W. (2014). featureCounts: an efficient general purpose program for assigning sequence reads to genomic features. Bioinformatics *30*, 923–930.
49. Dobin, A., Davis, C.A., Schlesinger, F., Drenkow, J., Zaleski, C., Jha, S., Batut, P., Chaisson, M., and Gingeras, T.R. (2013). STAR: ultrafast universal RNA-seq aligner. Bioinformatics *29*, 15–21.
50. Avanzato, D., Pupo, E., Ducano, N., Isella, C., Bertalot, G., Luise, C., Pece, S., Bruna, A., Rueda, O.M., Caldas, C., et al. (2018). High USP6NL Levels in Breast Cancer Sustain Chronic AKT Phosphorylation and GLUT1 Stability Fueling Aerobic Glycolysis. Cancer Res. *78*, 3432–3444.